EXCITATION FUNCTION OF NEUTRON INDUCED REACTION ON BARIUM ISOTOPES FOR NEUTRON ENERGIES BELOW 20MEV

By

Kebede Shogile

SUBMITTED IN PARTIAL FULFILLMENT OF THE
REQUIREMENTS FOR THE DEGREE OF
MASTER OF SCIENCE IN PHYSICS
(NUCLEAR PHYSICS)
AT
JIMMA UNIVERSITY
COLLEGE OF NATURAL SCIENCES
JIMMA,ETHIOPIA
JUNE 2018

JIMMA UNIVERSITY

PHYSICS

The undersigned hereby certify that they have read and recommend to the College of Natural Sciences for acceptance a thesis entitled "**Excitation Function of Neutron Induced Reaction on Barium Isotopes for Neutron Energies Below 20MeV**" by **Kebede Shogile** in partial fulfillment of the requirements for the degree of **Master of Science in Physics(Nuclear Physics)**.

Dated: <u>June 2018</u>

Supervisor: _____
Teklemariam Tessema (Phd)

External Examiner: _____
Pr.A.K. Chaubey

Internal Examiner: _____
Mr.Chali Yadeta

Chairperson: _____

JIMMA UNIVERSITY

Date: **June 2018**

Author: **Kebede Shogile**

Title: **Excitation Function of Neutron Induced Reaction on Barium Isotopes for Neutron Energies Below 20MeV**

Department: **Physics**

Degree: **MSc.**
Convocation: **June**
Year: **2018**

Permission is herewith granted to Jimma University to circulate and to have copied for non-commercial purposes, at its discretion, the above title upon the request of individuals or institutions.

_____
Signature of Author

Table of Contents

List of Tables

List of Figures

Abstract

In this work, neutron induced reactions on barium nucleus ($^{134}_{56}Ba - ^{136}_{56}Ba$) in different energy regions were theoretically studied. The nuclear reaction cross sections for five reactions namely, $^{134}Ba(n,2n)^{133}Ba$, $^{136}Ba(n,2n)^{135}Ba$, $^{134}Ba(n,p)^{134}Cs$, $^{135}Ba(n,p)^{135}Cs$ and $^{136}Ba(n,p)^{136}Cs$ were calculated using COMPLET nuclear computer code. Experimental cross section data was downloaded from the Experimental Nuclear Reaction Data library (EXFOR) for the reactions and energy ranges. This was based on the objective to compare the theoretically calculated data with experimental data. The data was compared using Figures and Tables followed by discussions. A good agreement is obtained between theoretically calculated cross section values and experimentally calculated cross section values for five reactions.

Acknowledgements

Chapter 1

Introduction

1.1   Background

The accurate knowledge of the nuclear reaction cross-sections and the excitation functions of fast neutron reactions are of interest from the point of view of nuclear reaction theory(nuclear models),fission and fusion reactor technology, fast reactor design and control calculations ,neutron fluence monitoring, safeguards, neutron therapy, medical physics, activation and prompt radiation analysis, radionuclides production and applications of data in dosimetry. Measurements of fast neutrons reactions cross-sections were carried out by various authors[1].

Barium is the fifth element in group 2(IIA) of the alkali earth metals and has most of the properties and characteristics of the other alkali earth metals in this group. It has 56 atomic number. Barium is a silvery metal that is somewhat malleable and machineable (can be worked on a lathe, stretched and pounded). Its melting point is 725^0c , its boiling point is about 1640^0c , and its density is $3.51\frac{g}{cm^3}$. The accurate figures for its properties are difficult to determine because of bariums extreme activitythe pure metal will ignite when exposed to air, water, ammonia, oxygen, and

the halogens. There are currently 35 known isotopes of barium, ranging from ^{120}Ba to ^{148}Ba. Seven of these isotopes are stable. The percentages of each as found in nature are as follows: $^{130}Ba = 0.106\%, ^{132}Ba = 0.101\%, ^{134}Ba = 2.147\%, ^{135}Ba = 6.592\%, ^{136}Ba = 7.854\%, ^{137}Ba = 11.23\%, and ^{138}Ba = 71.7\%$[2].

In this thesis, we calculated theoretically neutron induced reaction cross section as a function of energy on isotopes of barium in the energy range (13-15)MeV for the reactions $^{134}_{56}Ba(n,2n)^{133}_{56}Ba$, $^{136}_{56}Ba(n,2n)^{135}_{56}Ba$, and $^{134}_{56}Ba(n,p)^{134}_{55}Cs$, $^{135}_{56}Ba(n,p)^{135}_{55}Cs$ and $^{136}_{56}Ba(n,p)^{136}_{55}Cs$ between energy range $(1-20)$MeV. We selected energy below 20MeV.

1.2   Statement of the Problem

Explanation of the experimental work by theory and the explanation of theory by experimental work is needed for better justification of scientific discoveries. We didn't find published work on theoretical calculation of excitation function of neutron induced reaction on barium isotopes for the reaction (n,2n) between energy range (13 - 15)MeV and (n,p) between energy range $(1-20)$MeV. In this work theoretical calculation of excitation function of neutron induced reaction on isotopes of barium for the reaction (n,2n) between energy range $(13-15)$MeV and (n,p) reaction between energy range $(1-20)$MeV have been done. The following were the leading questions for the research.

- What are the theoretical values of reaction cross section of the neutron induced reaction on the isotopes of barium for the reactions $^{134}Ba(n,2n)^{133}Ba$ and $^{136}Ba(n,2n)^{135}Ba$ in between energy range $(13-15)$MeV?

- What are the theoretical values of reaction cross section of the neutron induced reaction on isotopes of barium for the reactions $^{134}Ba(n,p)^{134}Cs$, $^{135}Ba(n,p)^{135}Cs$ and $^{136}Ba(n,p)^{136}Cs$ in between energy range $(1-20)$MeV?

- How is the validity of the theoretically calculated data with respect to experimental data?

1.3   Objectives

1.3.1   General Objective

The general objective of the study was theoretical calculation of excitation function of neutron induced reaction on barium isotopes for the neutron energy below 20MeV

1.3.2   Specific Objectives

The specific objectives of the study were the following:

- To calculate theoretical reaction cross section of neutron induced reaction on isotopes of barium for the reactions $^{134}Ba(n,2n)^{133}Ba$ and $^{136}Ba(n,2n)^{135}Ba$ in between energy range $(13-15)$MeV.

- To calculate reaction cross section of neutron induced reaction on barium isotopes for the reactions $^{134}Ba(n,p)^{134}Cs$, $^{135}Ba(n,p)^{135}Cs$ and $^{136}Ba(n,p)^{136}Cs$ in between energy range $(1-20)$MeV.

- To describe theoretically calculated cross section values with experimentally calculated cross section values

1.4   Scope of the study

In this work, we focused only on the theoretical calculation of reaction cross section for the neutron induced reaction on barium isotopes for the reactions $^{134}_{56}Ba(n, 2n)^{133}_{56}Ba$ and$^{136}_{56}Ba(n, 2n)^{135}_{56}Ba$ between energy range $(13 - 15)$MeV and for the reactions $^{134}_{56}Ba(n, p)^{134}_{55}Cs$, $^{135}_{56}Ba(n, p)^{135}_{55}Cs$ and $^{136}_{56}Ba(n, p)^{136}_{55}Cs$ between energy range $(1 - 20)$MeV using exciton mode. Available theoretical and experimental works on the related fields were Compiled.

1.5   Significance

The main advantages that could be obtained from the study were:

- To find theoretical calculation of the reaction cross section for neutron induced reaction on isotopes of barium for the reactions $^{134}_{56}Ba(n, 2n)^{133}_{56}Ba$, $^{136}Ba(n, 2n)^{135}Ba$ between energy range $(13-15)$MeV and $^{134}Ba(n, p)^{134}Cs$, $^{135}Ba(n, p)^{135}Cs$ and $^{136}Ba(n, p)^{136}Cs$ between energy range $(1 - 20)$MeV.

- To give theoretical explanation of the reactions in comparison with the experimental results

- To support as a reference for further study in the area.

- To get better insight and information by the student working on the research.

Chapter 2

Literature Review

2.1 Nuclear Reaction

A nuclear reaction is a process that occurs when a nuclear particle (nucleon or nucleus) gets into close contact with another. Most of the known nuclear reactions are produced by exposing different materials to a beam of accelerated nuclear particles. Usually a strong energy and momentum exchange takes place and the final products of the reaction are one, two, or more nuclear particles leaving the point of close contact in various directions. The products are mostly of a species different from the particles in the original pair. We shall consider nuclear reactions of the type

$$a + X \rightarrow Y + b \tag{2.1.1}$$

or, in more compact notation, X(a,b)Y. The notation means that particle a strikes nucleus X to produce nucleus Y and an outgoing particle b. "Particles" a and b may be elementary particles (neutrons, protons), but they can also themselves be nuclei (e.g., deuterons or alpha-particles). Reaction (2.1.1) is not the most general nuclear reaction. In the general case, an arbitrary number of particles may emerge. This reaction is sufficiently general to include most of the known nuclear reactions

at low energy. There is one exception to this, however. We shall be interested in the radiative capture process, where X and a stay together to form a nucleus W while a gamma-ray is emitted:

$$a + X \rightarrow W + \hbar\omega \qquad (2.1.2)$$

We might have included this as a reaction of type (2.1.1), provided that we considered the gamma-ray a particle of the same type as a. However, there is good reason for not doing this. The interaction between nuclei and gamma-rays is weak and can be treated as a small perturbation, where as the interaction of nuclear projectiles (neutrons, protons, deuterons, etc.) with nuclei cannot be treated in that way. Furthermore in (2.1.2) the number of "particles" does not stay constant throughout the reaction if we admit $\hbar\omega$ as a particle-the gamma-ray is created during the process. For both these reasons (2.1.2) will be treated separately from reactions of type (2.1.1). The inverse reaction to (2.1.2) is called the photonuclear effect (in analogy to the photoelectric effect). We are usually interested in the probability of processes of type (2.1.1) or (2.1.2) as a function of the energy of the incident particle a, in the energy and the direction of the outgoing particles [3].

It was in the latter way that Rutherford observed, in 1919, the first nuclear reaction produced in laboratory,

$$\alpha + {}^{14}_{7}N \rightarrow {}^{17}_{8}o + p \qquad (2.1.3)$$

using -particles from a ^{214}Bi sample. As in eq. 2.1.3, other reactions were induced using α- particles, the only projectile available initially. With the development of accelerators around 1930, the possibilities multiplied by changing the energy and mass of the projectile. Today it is possible to bombard a target with protons of energy greater than 1TeV ($1TeV = 10^{12}eV = 1.602 * 10^7$ joules), and beams of particles as

heavy as uranium are available for study of reactions with heavy ions [4].

2.2   Reaction Mechanisms

Nuclear reactions may entail three types of reaction mechanisms: direct, compound nucleus and pre-equilibrium effects. The contribution of these processes depends on the given reaction and the energy of the incident particle. The three types can be distinguished by their angular distributions and time scales.

2.2.1   Direct Reaction

For projectile energies above $50MeV$ and for light target nuclei $A < 30$ a direct transition from the entrance to the exit channel occurs within a very short timescale of about 10^{-22} seconds, which is roughly the time it takes to traverse the nuclear field. There is no creation and subsequent decay of a highly excited intermediate state, which results in an anisotropic and forward-peaked angular distribution. Typical examples of direct reactions are elastic and inelastic scattering, charge transfer, stripping, pick-up, and knock-on processes.

Existence of such direct reactions was established by Butler" in 1950 from the angular distributions of (d, p)reactions. The loose structure of the deuteron makes the chance of interaction without compound nucleus formation especially high for this class of reactions. Austern, Butler, and Mc Manus later proposed a similar interpretation for (n , p) reactions. In both treatments, direct processes were considered to occur only when colliding nuclei graze each other, i.e., they were considered to be "surface" phenomena. It has since become apparent from the work of Hayakawa, Kawai,

and Kikuchi and of Brown and Muirhead, that this view point may at least ln the (n ,p) case, be too restrictive. Rather, it appears that direct reactions may originate in the volume of the target nucleus as well as at the edge. Although existence of direct mechanisms for reactions has been established beyond doubt, it seems that they account for only small fractions of most total cross sections, except when peculiar circumstances exaggerate their contribution relative to the compound nucleus one [5].

2.2.2 Compound Nucleus Reactions

Most of the low energy nuclear reactions follow this mechanism, which was first described by Bohr. The incident particle is captured to form a highly excited intermediate state C^*, whereby the energy of the projectile is distributed over all nucleons.

$$A + x \rightarrow C^* \rightarrow B + y$$
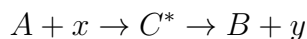
The compound nucleus decays by evaporation of nucleons with a Maxwellian energy distribution. The emission is symmetric to 90^0 and the interaction time is about 10^{-14} to 10^{-18} seconds.

2.2.3 Pre-compound or pre-equilibrium Reactions

On a time scale this process lies between the direct and the compound nucleus reactions. The particle is emitted before the energy is evenly distributed over all nucleons, thus giving a smooth forward-peaked angular distribution. Another characteristic is a pronounced high-energy tail in the excitation function [6].
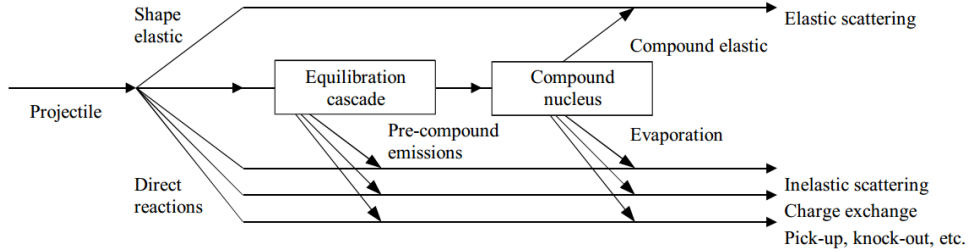
Figure 2.1: Reaction mechanisms in nuclear reaction

Energetics

The number of nucleons, the charge, energy, momentum, angular momentum, parity and isospin are preserved. The released energy of a nuclear reaction is the so called Q-Value, which can be calculated from the nuclide masses M_i and the speed of light c:

$$Q = (M_A + M_x - M_B - My) * c^2 \qquad (2.2.1)$$

A positive Q-Value denotes an exo-energetic reaction, while for endo-energetic reactions the Q-Value is negative. In the latter case the projectile has to deliver the necessary excitation energy. Taking into account also the conservation of momentum, we obtain the minimum energy which is required to initiate the nuclear reaction, the threshold energy:

$$E_{thres} = -Q * (1 + \frac{M_x}{M_A}) \qquad (2.2.2)$$

where M_x and M_A are the masses of the projectile and target nucleus, respectively.

Reaction Channels

For a given particle energy different reactions are possible depending on the Q-Values. In the investigated energy range up to about $21 MeV$, these so called reaction channels are, for example, elastic and inelastic scattering, neutron capture, charged particle

emission and multiple neutron emission.

$$a + X = \begin{cases} X + a \\ X^* + a \\ Y + b \\ Z + c \\ etc, \end{cases} \qquad (2.2.3)$$

The first two reactions (2.2.3) are distinguished by the fact that the projectile a re-emerges after the reaction. The first of these represents elastic scattering. The first of these represents elastic scattering: the projectile a leaves with the same energy (in the center-of-gravity system), and the target nucleus X is left in its initial state. The second reaction represents inelastic scattering: the target nucleus X is forced into an excited state X^*, and the projectile a re-emerges, but with an energy lower than its initial one by the amount of the excitation energy given to the target nucleus [7].

All the reactions (2.2.3), except the elastic scattering, can be subdivided again according to the quantum state of the residual nucleus and the emerging particle. We denote the states of the nuclei by $\alpha', \beta', \gamma', \dots$, and the states of the incident or emerging particles by $\alpha'', \beta'', \gamma'', \dots$ If particles a, b, etc., are elementary, states α'', β'', etc., refer to their spin orientation. We get the reactions

$$a''_\alpha + X'_\alpha = \begin{cases} X'_\alpha + a''_\alpha \\ X'_\beta + a''_\beta \\ Y'_\gamma + b''_\gamma \\ etc, \end{cases} \qquad (2.2.4)$$

Here α' and α'' are states of the target nucleus and the incident particle, β' and β'' , or γ' and γ'' , can denote any quantum state of X and a. or Y and b, respectively,

10

which can be created in this reaction. Of course, the conservation laws of energy, angular momentum, and parity restrict the possible pairs of β' and β'', γ' and γ'', etc. Any such possible pair of residual nucleus and emerging particle, each in a definite quantum state, is called a reaction channel. We shall denote channels by single Greek letters, $\alpha, \beta, ...$, which comprise both indices α' and α'', or β'. Channel $X_\alpha + a''_\alpha$ is called the entrance channel or initiating channel of reaction (2.2.4).

2.3   Interaction of Neutron With Nuclei

The free neutron is unstable against β decay with half life of $10.6min$. In nuclei the bound neutron may be much longer lived (even stable) or much shorter lived. Despite the instability of free neutrons, their properties are measured to high precision, particularly the magnetic dipole moment $\mu = -1.91304184 \pm 0.00000088\mu_N$ and the neutron-proton mass difference, $m_n - m_p = 1.29340 \pm 0.00003 MeV$[8].

Neutrons have proven to be especially effective in producing nuclear transformation. Since they have no electric charge, they are not subject to repulsive electrostatic forces in the neighborhood of positively charged nucleus, and are therefore more likely to penetrate nuclei than are protons, deuterons, or alpha particles. Not only are highly energetic neutrons capable of causing nuclear reactions, but slowly moving neutrons are also extremely effective. Because of these properties of the neutron many more disintegrations have been produced with neutrons than with any other particle [9].

The first experimental observation of the neutron occurred in 1930, when Bothe and Becker bombarded Beryllium with alpha particles (from radioactive decay) and obtained a very penetrating and indirectly ionizing radiation, which they assumed to be γ ray. Soon thereafter, Curie and Juliot noticed that when this radiation

fell on paraffin an energetic protons were emitted. From the range of these protons they determined their energy to be $5.3MeV$. They computed that the energy of this 'radiation' would be at least $52MeV$ to release such protons. An emitted γ of such an energy seemed extermely unlikely. In 1932, James Chadwick provided the correct explanation, identifying the unknown radiation as a neutral(therefore penetrating and indirectly ionizing) particle with a mass nearly the same as that of proton. James Chadwick did additional recoil experiment's with neutrons and confirmed his hypothesis, and he is generally credited with being the discoverer of the neutron [8].

Since its discovery by James Chadwick in February 1932, the neutron has changed the world of nuclear physics and eventually the course of human history. Not even a month passed by when in March 1932 at the Cavendish Laboratory in Cambridge, using for the first time neutrons as projectiles, it was observed that a neutron colliding with a nucleus of nitrogen could disintegrate it; two years later, in March 1934, Enrico Fermi earned his Nobel Prize discovering the possibility to induce artificial radioactivity with neutrons. Appointed Professor of Physics at Columbia University, New York, in 1939, Fermi continued his studies on neutrons; thanks to the discovery of fission, by Hahn and Strassmann, Meitner and Frish in 1939, Fermi obtained the first controlled nuclear chain reaction, on a squash court situated beneath Chicagos stadium, in December 1942. The Manhattan Project boosted the investigation of neutron induced reactions. At the end of the Second World War, energy production became a second important driving force of neutron research, along with military applications. Others fields of study on neutron induced reactions include radiation treatment of cancer and neutron-induced nucleo-synthesis in astrophysics [10].

Neutrons can cause many different types of interactions. The neutron may simply scatter off the nucleus in two different ways, or it may actually be absorbed into the nucleus. If a neutron is absorbed into the nucleus, it may result in the emission of a gamma ray or a subatomic particle, or it may cause the nucleus to fission.

A neutron scattering reaction occurs when a nucleus, after having been struck by a neutron, emits a single neutron. Despite the fact that the initial and final neutrons do not need to be (and often are not) the same, the net effect of the reaction is as if the projectile neutron had merely "bounced off," or scattered from, the nucleus. The two categories of scattering reactions, elastic and inelastic scattering, are described in the following paragraphs.

In an elastic scattering reaction between a neutron and a target nucleus, there is no energy transferred into nuclear excitation. Momentum and kinetic energy of the "system" are conserved although there is usually some transfer of kinetic energy from the neutron to the target nucleus. The target nucleus gains the amount of kinetic energy that the neutron loses. Elastic scattering of neutrons by nuclei can occur in two ways. The more unusual of the two interactions is the absorption of the neutron, forming a compound nucleus, followed by the re-emission of a neutron in such a way that the total kinetic energy is conserved and the nucleus returns to its ground state. This is known as resonance elastic scattering and is very dependent upon the initial kinetic energy possessed by the neutron. Due to formation of the compound nucleus, it is also referred to as compound elastic scattering. The second, more usual method, is termed potential elastic scattering and can be understood by visualizing the neutrons and nuclei to be much like billiard balls with impenetrable surfaces. Potential scattering takes place with incident neutrons that have an energy of up to

about 1MeV. In potential scattering, the neutron does not actually touch the nucleus and a compound nucleus is not formed. Instead, the neutron is acted on and scattered by the short range nuclear forces when it approaches close enough to the nucleus.

In inelastic scattering, the incident neutron is absorbed by the target nucleus, forming a compound nucleus. The compound nucleus will then emit a neutron of lower kinetic energy which leaves the original nucleus in an excited state. The nucleus will usually, by one or more gamma emissions, emit this excess energy to reach its ground state. For the nucleus that has reached its ground state, the sum of the kinetic energy of the exit neutron, the target nucleus, and the total gamma energy emitted is equal to the initial kinetic energy of the incident neutron. Most absorption reactions result in the loss of a neutron coupled with the production of a charged particle or gamma ray. When the product nucleus is radioactive, additional radiation is emitted at some later time. Radiative capture, particle ejection, and fission are all categorized as absorption reactions and are briefly described below. In radiative capture the incident neutron enters the target nucleus forming a compound nucleus. The compound nucleus then decays to its ground state by gamma emission.

In a particle ejection reaction the incident particle enters the target nucleus forming a compound nucleus. The newly formed compound nucleus has been excited to a high enough energy level to cause it to eject a new particle while the incident neutron remains in the nucleus. After the new particle is ejected, the remaining nucleus may or may not exist in an excited state depending up on the mass-energy balance of the reaction. One of the most important interactions that neutrons can cause is fission, in which the nucleus that absorbs the neutron actually splits into two similarly sized parts [11].

2.4 Reaction cross section

The cross-sections for various nuclear reactions depend on the bombarding energy of the incident particle in a highly individualistic manner. The detailed dependence of cross-sections on bombarding energy is often called the "excitation function" or the "transmutation function" for the particular reaction. The shape of some excitation functions can be explained with these competing reaction channels: a steep rise near the threshold followed by a plateau and then a decrease at energies, where other reactions become energetically possible. The contributions of different channels to the total cross section depend also on the mass region. For heavier nuclei and thus higher nuclear charge, for example, the emission of charged particles is increasingly suppressed due to the increasing Coulomb barrier. A nuclear reaction $A(x, y)B$ occurs, when a projectile x comes sufficiently close to the target nucleus A, i. e. closer than the range of the nuclear forces $(10^{-14}m)$. The interaction of the projectile with the target nucleus is generally described in terms of the cross section $\sigma_{x,y}$, which is a measure of the probability for a reaction to occur. The cross section is usually given in barns $(1b = 10^{-28}m^2 = 10^{-24}cm^2)$ and is a function of the energy of the incident particle. The plot of $\sigma(E)$ against E is called the excitation function [1].

A characteristic feature of neutron-induced reactions is the existence of a well-defined total cross section ,which is the sum of the elastic scattering cross section and the reaction cross section. The total cross section is ill defined in reactions induced by charged particles, since it contains the Rutherford scattering cross section which becomes extremely large for very small scattering angles. The scattering through very small angles is determined by the Coulomb field far outside the nuclear surface and depends critically on the shielding of the nuclear charge by the atomic electrons.

Hence the total cross section in the case of charged particles is mostly an atomic phenomenon [3].

Geometrical Limitations on Reaction and Scattering Cross Sections

Consider a beam of particles directed at a layer of matter. In most nuclear reactions the effect of this layer is composed additively of the effects of individual units (scattering centers) in the layer; the individual nuclei in the material act as independent scattering centers. The cross section of a reaction is then defined by

$$\sigma = \frac{number\,of\,events\,of\,given\,type\,per\,unit\,time\,per\,nucleus}{number\,of\,incident\,particles\,per\,unit\,area\,per\,unit\,time} \qquad (2.4.1)$$

The concept of a cross section cannot be used if large numbers of nuclei act coherently. This occurs in only one type of nuclear reaction: the scattering (but not the absorption) of a beam of very slow neutrons by crystalline material. In all other cases the cross section (2.4.1) has a well-defined meaning.

Let us consider a plane wave of particles a incident upon the nucleus X, representing an entrance channel α. Particle a can be re-emitted into the same channel, or it can initiate a nuclear reaction which leads into another channel. We shall separate the elastic scattering events from all the other reactions (2.2.3) and from (2.1.2), so that the total cross section $\sigma_t(\alpha)$ for all events which may take place is given by

$$\sigma_t(\alpha) = \sigma_{sc}(\alpha) + \sigma_r(\alpha) \qquad (2.4.2)$$

Here $\sigma_{sc}(\alpha)$ denotes the elastic scattering cross section, and $\sigma_r(\alpha)$ denotes the combined cross section for all events other than elastic scattering. (We include the various inelastic scattering cross sections in $\sigma_r(\alpha)$) We shall refer to $\sigma_r(\alpha)$ as the " reaction cross section."

16

We assume for the sake of simplicity that target nucleus X, as well as projectile a, has zero spin. This assumption is correct only if we use alpha-particles as projectiles, and nuclei with even A as targets. It is certainly incorrect for neutron or proton reactions. Most of the results, however, are not affected by this assumption, which greatly simplifies the treatment.

We can break up each channel α into sub channels (α, l) with given orbital angular momentum l. It is useful to decompose the incident plane wave into spherical harmonics; each spherical harmonic $Y_{l,0}(\theta)$ in this expansion corresponds to a spherical wave in the particular entrance sub-channel (α, l). The cross sections can also be subdivided into partial cross sections:

$$\sigma_{sc}(\alpha) = \sum_{l=0}^{\infty} \sigma_{sc,l} \qquad \sigma_r(\alpha) = \sum_{l=0}^{\infty} \sigma_{r,l} \qquad (2.4.3)$$

where $\sigma_{sc,l}$ and $\sigma_{r,l}$ are the cross sections for the reactions and the elastic scattering events initiated by incident particles with an angular momentum l. σ_l is defined by (2.2.1) if the numerator contains terms corresponding only to those reactions or scattering events which are initiated by incident particles of given l, the denominator remaining the same. The separation (2.4.3) of the cross section into additive contributions of given l is possible only for the cross sections integrated over the angles of emergence of the reaction products.

The differential cross section for a reaction or scattering in which the emergent particle leaves in a definite direction θ involves interference terms between the contributions from different values of l, since definite phase relations between these contributions exist in the incident plane wave. These interference terms vanish after the integration over the full solid angle.

Geometrical considerations show that there are upper bounds for the partial reaction

cross sections $\sigma_{r,l}$. Before deriving the value of these bounds, we give a crude argument for their existence. The significance of the angular momenta in a plane wave can be visualized by dividing up the incident beam into cylindrical zones (see Fig. 2.2). The innermost zone contains particles with impact parameters less than $\bar{\lambda} = \frac{\lambda}{2\pi}$ (λ = de Broglie wavelength of the relative motion). The next zone contains all particles with impact parameters between $\bar{\lambda}$ and $2\bar{\lambda}$. The lth zone contains particles with impact parameters between $l\bar{\lambda}$ and $(l+1)\bar{\lambda}$. Then, according to elementary classical mechanics, the incident particles moving in the lth zone have angular momenta (i.e., momentum X impact parameter) between $Mvl\bar{\lambda}$ and $Mv(l+\bar{\lambda})$, i.e., between $\hbar l$ and $\hbar(l+1)$. In quantum mechanics only integral values l of the angular momentum are admitted. It might be thought that this quantization of angular momenta implies also quantization of impact parameters (i.e., motion of the particles only with definite, quantized impact parameters). This interpretation is too rigid, since it is
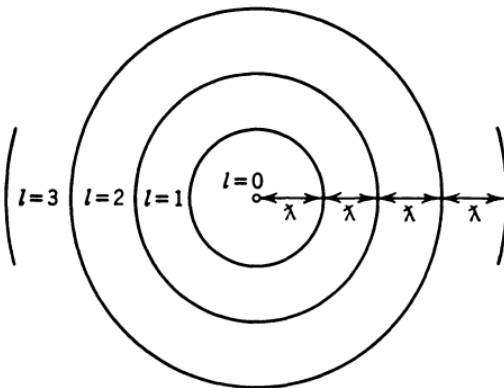
Figure 2.2: The incident beam is directed perpendicular to the plane of the figure.

impossible to speak of a well-defined impact parameter in a beam whose particles have a well-defined velocity. However, it is approximately correct to assume that the particles with an angular momentum l move in the lth zone. The cross-sectional area

18

of the lth zone is $(2l+1)\pi\bar{\lambda}^2$. Since no more particles can be taken out of the beam than are in it originally, we expect that the reaction cross section $\sigma_{r,l}$ cannot be larger than this amount, i.e.,

$$\sigma_{r,l} \leq (2l+1)\pi\bar{\lambda}^2 \tag{2.4.4}$$

It should be noted that (2.4.4) does not apply to the scattering cross section.

We now proceed to give a more formal derivation of (2.4.4). The incident beam is represented by a plane wave in the incident channel. We define the channel coordinate r_α as the vector between the center of the target nucleus X and the projectile a. The plane wave can be written in the form

$$exp(ik_\alpha * r_\alpha) = exp(ikz)$$

if we choose the z-axis parallel to k_α. The wave vector k_α is related to the relative velocity $V_\alpha = \dot{r}_\alpha$ by

$$k_\alpha = \frac{M_\alpha V_\alpha}{\hbar} \qquad M_\alpha = \frac{M_a M_x}{M_a + M_x} \tag{2.4.5}$$

where the "channel mass" M_α is the reduced mass of a and X. The channel wave number $k_\alpha = |k_\alpha|$ and the channel wavelength $\bar{\lambda}_\alpha$ are related to the channel energy ϵ_α by

$$k_\alpha = \frac{1}{\bar{\lambda}_\alpha} = \frac{(2M_\alpha\epsilon_\alpha)^{\frac{1}{2}}}{\hbar} \tag{2.4.6}$$

The plane wave can be expanded into spherical harmonics. For large values of kr this expansion becomes (we drop the index α in the rest of this section)

$$exp(ikz) \cong \frac{\pi^{\frac{1}{2}}}{kr} \sum_{l=0}^{\infty} \sqrt{2l+1}i^{l+1}\{exp[-i(kr - \frac{1}{2}l\pi)] - exp[+i(kr - \frac{1}{2}l\pi)]\}Y_{l,0} \tag{2.4.7}$$

This expression describes an undisturbed plane wave. The nuclear reaction changes this expression. However, only the outgoing wave which is proportional to $exp(ikr)$ is

19

changed. Hence the actual wave function in the incident channel has an asymptotic behavior differing from (2.4.7) in the coefficient of $exp(ikr)$ only. We write for the wave function in the incident channel, for $kr >> 1$,

$$\psi(r) \cong \frac{\pi^{\frac{1}{2}}}{kr} \sum_{l=0}^{\infty} \sqrt{2l+1} i^{l+1} \{exp[-i(kr - \frac{1}{2}l\pi)] - \eta_l exp[+i(kr - \frac{1}{2}l\pi)]\} Y_{l,0} \quad (2.4.8)$$

where the complex number η_l is the coefficient of the outgoing wave with angular momentum l. The scattered wave ψsc is the difference between the actual wave (2.4.8) and the incident wave (2.4.7):

$$\psi_{sc} = \psi(r) - exp(ikz) = \frac{\pi^{\frac{1}{2}}}{kr} \sum_{l=0}^{\infty} \sqrt{2l+1} i^{l+1} (1 - \eta_l) exp[+i(kr - \frac{1}{2}l\pi)] Y_{l,0} \quad (2.4.9)$$

We obtain the scattering cross section by dividing the number N_{sc} of scattered particles per second by the number N of the incident particles per square centimeter per second. In order to find N_{sc} we enclose the center by a large sphere of radius r_0 and equate N_{sc} to the flux of ψsc through this sphere:

$$N_{sc} = \frac{\hbar}{2iM} \int (\frac{\partial \psi}{\partial r} \psi_{sc}^* - \frac{\partial \psi_{sc}^*}{\partial r} \psi_{sc}) r_0^2 \sin\theta d\theta d\varphi \quad (2.4.10)$$

where the integral is extended over the surface of the sphere. Because of the orthogonality and normalization of the $Y_{l,0}$ we get

$$N_{sc} = \frac{v\pi}{k^2} \sum_{l=0}^{\infty} (2l+1)|1 - \eta_l|^2$$

where v is the velocity of the particles. The value of the flux N in a plane wave $exp(ikz)$ is equal to the velocity v, so that we get for the scattering cross section

$$\sigma_{sc,l} = \pi \bar{\lambda}^2 (2l+1)|1 - \eta_l|^2 \quad (2.4.11)$$

The reaction cross section is determined by the number N_a of particles taken out of the beam per second. N_a is the number of particles which enter a sphere of radius

r_0 around the center without leaving it again through the entrance channel. It is therefore equal to the net flux into this sphere as computed from the complete wave function ψ (2.4.8):

$$N_a = -\frac{\hbar}{2iM}\int(\frac{\partial\psi}{\partial r}\,\psi^* - \frac{\partial\,\psi^*}{\partial r}\psi)r0^2\sin\theta d\theta d\varphi \qquad (2.4.12)$$

(The minus sign in front makes the influx N_a positive.) The reaction cross section σ_r is given by $\frac{N_a}{N}$; thus the contribution of the lth sub-wave is

$$\sigma_{r,l} = \pi\bar{\lambda}^2(2l+1)(1-|\eta_l|^2) \qquad (2.4.13)$$

Equation (2.4.13) provides the formal proof of the geometrical limit (2.4.4) on the reaction cross section, since $|\eta_l|^2$ can never be negative. Furthermore, unless $|\eta_l|^2$ is smaller than or equal to unity, the outgoing wave in (2.4.8) has a higher intensity than the incoming one. The condition

$$|\eta_l|^2 \leq 1$$

insures that the cross section (2.4.13) does not become negative. Inspection of (2.4.11) and (2.4.12) leads to an inequality connecting $\sigma_{sc,l}$ and $\sigma_{r,l}$. To get the largest possible scattering cross section we must put $\eta_l = 1$, and this implies that $\sigma_{r,l}$ vanishes. On the other hand, we get the maximum amount removed from the beam when we put $\eta_l = 0$, and this implies $\sigma_{sc,l} = \sigma_{r,l} = (2l+1)\pi\bar{\lambda}^2$. This is precisely the limiting value (2.4.4) found qualitatively before. In general, for any given scattering cross section there is a maximum value of the reaction cross section. Any reaction is equivalent to an absorption of the incident wave in the entrance channel. The reaction may lead to an emission of the particle in another channel. It is an absorption as far as the entrance channel is concerned. Any absorption consists of a weakening of the outgoing part of the plane wave. This is equivalent to an addition to the plane wave of

an outgoing wave with a phase opposite to the one of the plane wave. This addition appears as a scattered wave. Scattering without absorption occurs if the outgoing part of the plane wave is not weakened in intensity but only shifted in phase. The maximum value of the scattering cross section is four times the maximum value of the reaction cross section. We see from (2.4.11) that the phase of η affects the magnitude of σ_{sc}, whereas only $|\eta|^2$ enters into σ_r .

The incoming and outgoing waves are coherent in elastic scattering. They can interfere, constructively or destructively.

The angular distribution of the scattered beam is also determined by the η_l. Let us ask for the cross section $\sigma_{sc}(\theta)d\Omega$ for the scattering into the solid angle element $d\Omega$, which includes the angle θ with the direction of the incident beam (z-direction). We determine the number $N_{sc}(\theta)d\Omega$ of particles scattered per second into $d\Omega$ by equating it to the flux through a surface element of the sphere of radius r_0:

$$N_{sc}(\theta)d\Omega = \frac{\hbar}{2iM}(\frac{\partial \psi sc}{\partial r} \ \psi* - \frac{\partial \ \psi sc*}{\partial r}\psi sc)r_0^2 d\Omega \tag{2.4.14}$$

This can be calculated from (2.4.9); we obtain, after division by the incident flux $N = v$,

$$\sigma_{sc}(\theta)d\Omega = \frac{\pi}{k^2}|\sum_{l=0}^{\infty}(2l+1)^{\frac{1}{2}}(1-\eta_l)Y_{l,0}(\theta)|^2 d\Omega \tag{2.4.15}$$

Here the contributions of different l 's interfere, so that it is no longer possible to write $\sigma_{sc}(\theta)$ as a sum of contributions each of which is due to a specified l.

The η_l do not determine the division of the reaction cross section into cross sections for the different reactions leading to the various open channels $\beta \neq \alpha$. We shall need separate assumptions to determine this subdivision. It is of interest to discuss the limiting case of a "black" nucleus whose radius R is much larger than the wavelength

$\bar{\lambda}$. We assume that all particles that strike the nucleus are absorbed by it and therefore lead to a reaction. According to our previous considerations, all particles with $l \leqslant \frac{R}{\bar{\lambda}}$ strike the nucleus. Our assumption therefore is expressed by

$\eta_l = 0$ as long as $lL < R$

$\eta_l = 1$ for larger values of l

Then equations (2.4.11) and (2.4.12) give

$$\sigma_r = \sigma_{sc} = \sum_{l=0}^{\frac{R}{\bar{\lambda}}} (2l + 1)\pi\bar{\lambda}^2 \cong \pi R^2$$

We thus obtain the apparently paradoxical result that the total cross section is twice the geometrical cross section of the nucleus:

$$\sigma_t = \sigma_{sc} + \sigma_r \cong 2\pi R^2 \tag{2.4.16}$$

This result has been confirmed experimentally. The seeming paradox may be explained by a consideration of the meaning of scattering [3].

2.5 Exciton model

Still modified and logically simple model is presented by Griffin. The exciton model for pre-equilibrium nuclear reactions has proven to be powerful for the analysis of continuum emission spectra and excitation functions for projectile energies above several MeV. It is imagined that the incident particle step-by-step creates more complex states of excited particles and holes in the compound system of target plus projectile and thereby gradually loses its memory of the initial energy and direction. Pre-equilibrium emission takes place after the first stage of the reaction but long before

statistical equilibrium of the compound nucleus is attained, leading to the well-known high-energy tails in the emission spectra and the smooth forward peaked angular distributions. The exciton model states that, at any moment during the reaction, the nuclear state is characterized by the total energy E^{tot} of the system and the total number of particles (p) above and holes (h) below the Fermi surface. In this model it is assumed that the incoming projectile, by interacting with the target nucleus, gives rise to a simple initial configuration characterized by a small number of excited particles and holes called excitons ($n = p + h$). Successive two-body residual interactions give rise to an intranuclear cascade through which a sequence of states characterized by an increasing exciton number, eventually leads to a fully equilibrated residual nucleus. Restriction to two-body residual interactions leads to the following selection rules concerning the possible variation of the number n of excitons, of particles p, and holes h:

$$\Delta n = 0, \pm 2; \Delta p = 0, \pm 1; \Delta h = 0, \pm 1. \tag{2.5.1}$$

The states which are excited in this interaction cascade are very unstable. The possible sequence of events considered in the exciton model. At each stage of this equilibrium process there is a competition between two decay modes of the composite nucleus: the decay by exciton-exciton interactions are more complex configurations and the decay by emission of particles into the continuum. The exciton model assumes that

1. At each stage of the cascade all of the states with the same configuration and the same total energy are equiprobable.

2. At each stage of the cascade all the processes which may occur are also equiprobable.

The first assumption gives the energy distribution of the excitons.

Two-component exciton model The two-component exciton formalism describes the evolution of a nuclear reaction in terms of the time-dependent population of so-called exciton states which are characterized by proton and neutron particle and hole numbers. We use a notation in which $p_\pi(p_\nu)$ is the proton (neutron) particle number and $h_\pi(h_\nu)$ the proton (neutron) hole number. We also define the proton exciton number $n_\pi = p_\pi + h_\pi$ and the neutron exciton number $n_\nu = p_\nu + h_\nu$. From this, we can construct the charge-independent particle number $p = p_\pi + p_\nu$, the hole number $h = h_\pi + h_\nu$ and the exciton number $n = n_\pi + n_\nu$. Two-body interactions allow transitions to occur from one exciton state to another. This is depicted schematically for a proton-induced reaction in Fig.2.3. The first and top-most state in the reaction chain is(1,0,0,0)(n=1). From this initial configuration two new configurations (n=3) may be populated in the first step: (2,1,0,0) by the creation of a new proton particlehole pair and (1,0,1,1) by the creation of a neutron particlehole pair. From the second step onwards, the particlehole configurations may decay by all types of possible exciton interactions, which in general are formulated as follows:
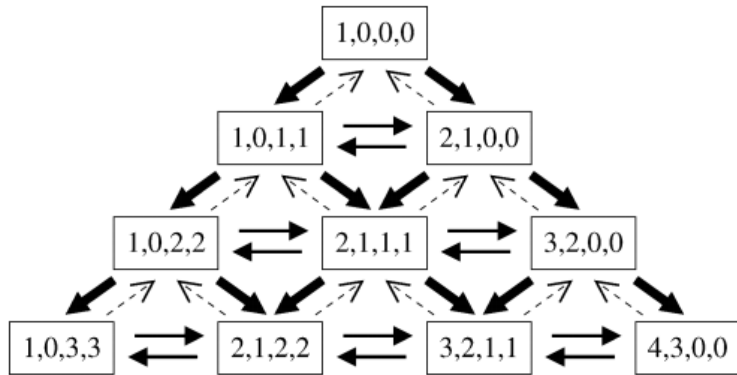
Figure 2.3: Schematics picture of the possible reaction pathways

25

- Further particlehole creation producing $(n + 1)$ -states, denoted by the thick arrows pointing downwards;

- Proton (or neutron) particlehole annihilation leading to a new neutron (proton) particlehole pair and, hence, to other n-states (the so-called pair conversion or charge exchange interaction), denoted by the open arrows pointing sideways;

- Proton (or neutron) particlehole annihilation yielding less complex $(n - 1)$ -states, denoted by the dashed arrows pointing upwards [12].

Chapter 3

Materials and Method

3.1 Materials

During the research work, the following materials and resources have been used.

- Computer code

- computer software

- References like journals, books, thesis and dissertation.

- Experimental data from Experimental Nuclear Reaction Data (EXFOR)

3.2 Method

Information from different reference materials have been compiled on experimental nuclear reaction cross section measurements about neutron induced reaction on barium isotopes particularly $(n, 2n)$ and (n,p) reactions. If available, information on theoretical calculations of cross section have also been visited. We had visited Calculations of (n,2n) reaction cross sections for barium isotopes from 5 to 20 MeV using TALYS 1.6, EMPIRE-3.2.2, and ALICE-GDH codes based on statistical model. Using

FORTRAN-77 based computer program called "COMPLET" numerical calculation of reaction cross section for the neutron induced reaction on barium isotopes particularly $(n, 2n)$ and (n,p) reactions for a given energy ranges of neutron were made. The "COMPLET" code used was discussed in Annex at the end.

The result of the cross section calculation were plotted against the neutron energy. At the last, the result had been compared with the experimental measurements.

Chapter 4

Result and Discussion

In this work, the neutron induced reaction cross section as a function of energy on isotopes of barium ($^{134}_{56}Ba-^{136}_{56}Ba$) for the reactions : $^{134}Ba(n,2n)^{133}Ba$, $^{136}Ba(n,2n)^{135}Ba$, $^{134}Ba(n,p)^{134}Cs$, $^{135}Ba(n,p)^{135}Cs$ and $^{136}Ba(n,p)^{136}Cs$ in different energy regions were theoretically calculated. The excitation functions of the reactions were depicted after the generation of data with the help of COMPLET code. The results of experimental cross sections were extracted from the EXFOR library for comparison with the theoretical values. For theoretical calculation all projectile energies used are the same with those used during the experimental work. During the data compiling theoretically, the input and output data were saved in a computer. After completion of compiling the theoretical cross section data for each of the five neutron induced reactions, the data were presented in Tables and Figures as shown below.

4.1 Excitation function of the reaction $^{134}Ba(n,2n)^{133}Ba$

4.1.1 Experimental Excitation Function

In 1988 Y.Ikeda ,C.konno, K.Oishi, T.Nakamura, H.Miyade, K.Kawade, H.Yamamoto and T.Katoh experimentally calculated reaction cross section values for the reaction

$^{134}Ba(n, 2n)^{133}Ba$ for the neutron energy from 13.34 to 14.93MeV. They measured the cross section for eight neutron energies i.e., 13.34MeV, 13.57MeV, 13.75MeV, 13.99MeV, 14.23MeV, 14.43MeV ,14.67MeV and 14.93MeV using Fusion neutronic source (FNS) facility as shown in the Table 4.1[13].

4.1.2 Theoretical Excitation Function

In a literature there have been a report on the theoretical calculation of reaction cross section for this reaction but not using COMPLET code. Halide Sahan, Muhittin Sahan and Eyyup Tel have calculated the excitation function of neutron induced reaction on barium isotopes of the reaction (n,2n) for the neutron energy region from 5 to 20MeV using TALYS 1.6, EMPIRE-3.2.2, and ALICE-GDH codes based on statistical model as given in the literature [14]. In this research, the values of neutron induced reaction cross sections were calculated with the help of COMPLET code as a function neutron energies for the reaction $^{134}Ba(n, 2n)^{133}Ba$ as given in the Table 4.1.

4.1.3 Comparison between experimental data and obtained data in this research

Table 4.1: Excitation function for the reaction $^{134}Ba(n, 2n)^{133}Ba$

$E_n(MeV)$	$\sigma - Experimental(mb)$	$\sigma - Theoretical(mb)$
13.34	682	680
13.57	736	674
13.75	764	864
13.99	754	859
14.23	766	832
14.43	834	823
14.67	795	817
14.93	829	991

As shown in Figure 4.1 the theoretical value of cross section is very close to the experimental value at 13.34 MeV and 14.43MeV neutron energies. However, the calculated values of cross section deviate from the experimental cross section values at 13.99MeV and 14.93MeV compared to other energies considered. The smallest cross section values were obtained for neutron energies 13.34MeV and 13.57MeV for experimental and theoretical data respectively. The maxima regions are the same for both the theoretical and experimental calculations. From this result, one can conclude that COMPLET code calculation data approaches the experimental value for the reaction on energy range 13.33 to 14.93MeV.
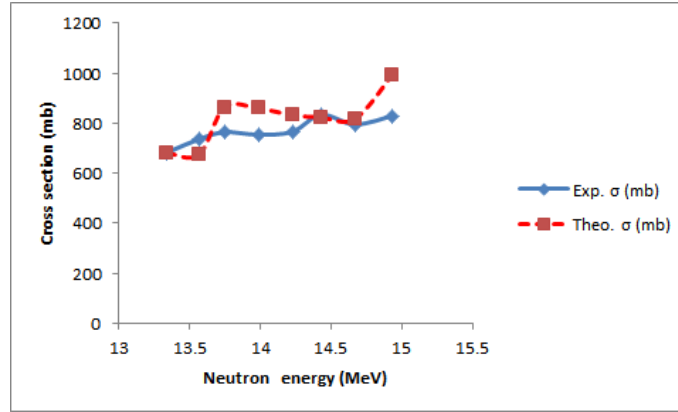
Figure 4.1: Excitation function for the reaction $^{134}Ba(n,2n)^{133}Ba$

4.2   Excitation function of the reaction $^{136}Ba(n,2n)^{135}Ba$

4.2.1   Experimental Excitation Function

In 1988 Y.Ikeda ,C.konno, K.Oishi, T.Nakamura, H.Miyade, K.Kawade, H.Yamamoto and T.Katoh experimentally calculated reaction cross section values for the reaction $^{134}Ba(n,2n)^{133}Ba$ for the neutron energy from 13.34 to 14.93MeV. They measured the cross section for eight neutron energies as given in the table using fusion neutronic

sources facility [13].

4.2.2 Theoretical Excitation Function

In this work, Cross section values were calculated as a function of neutron energy using FORTRAN-77 based nuclear reaction code called COMPLET. The theoretically calculated cross section data for the reaction were as displayed in Table 4.2 together with experimentally given data from EXFOR for each energy.

4.2.3 Comparison between experimental data and obtained data in this research

Table 4.2: Excitation function for the reaction $^{136}Ba(n, 2n)^{135}Ba$

$E_n(MeV)$	$\sigma - Experimental(mb)$	$\sigma - Theoretical(mb)$
13.33	851	840
13.56	868	934
13.75	863	830
13.98	910	826
14.22	879	797
14.43	912	967
14.67	939	960
14.93	946	953

Table 4.2 shows that there is a slight difference between theoretical and experimental values of reaction cross section. Closest values of theoretical and experimental cross section have been obtained at 14.93MeV and 13.33MeV neutron energies compared to other energy regions considered for the reaction. At 13.98MeV and 14.22MeV of neutron energies the two values of reaction cross sections are slightly far from each other compared to other energies considered. From this result one can conclude that COMPLET code calculation data approaches the experimental value for the reaction

on energies 13.33MeV , 13.56MeV ,13.75MeV, 13.98MeV, 14.22MeV , 14.43MeV , 14.67MeV and 14.93MeV.
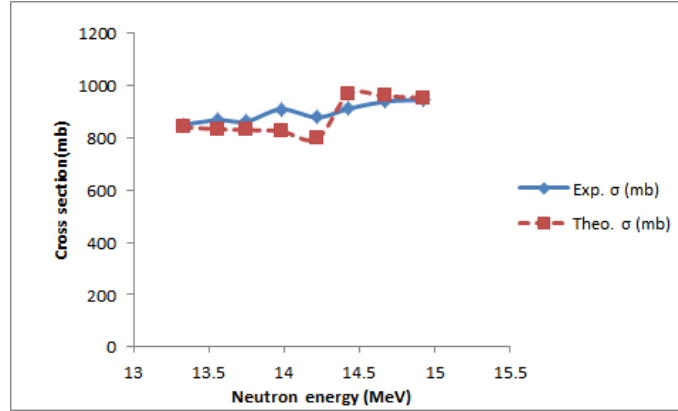
Figure 4.2: Excitation function for the reaction $^{136}Ba(n, 2n)^{135}Ba$

4.3 Excitation function of the reaction $^{134}Ba(n, p)^{134}Cs$

4.3.1 Experimental Excitation Function

B.Strohmaier, M.Uhl, W.K.Matthes experimentally calculated reaction cross section for the reaction $^{134}Ba(n, p)^{134}Cs$ in their work entitled as Application of nuclear reaction models for neutron nuclear data evaluation. statistical and optical model calculations for 134 - 138 barium. Average neutron-induced reaction cross sections for $^{134-138}Ba$ (the barium isotopes of mass number 134 through 138) for incident energies between 20keV and 20MeV have been calculated by means of the optical and the statistical model with consideration of pre-equilibrium emission. The calculations comprise the total, the nonelastic, the differential elastic, and the $(n, \gamma), (n, xn\gamma), (n, p\gamma), (n, pn\gamma),$ and (n, np) cross sections, as well as the production spectra of neutrons, protons, and gamma rays. For the model calculations, a consistent set of parameters based as much as possible on experimental data was employed [15].

4.3.2 Theoretical Excitation Function

With the support of COMPLET code cross section values were calculated theoretically for different neutron energies as shown with the support of Table 4.3. For neutron energies of 1-3MeV already there is no the probability of neutron induced reaction to take place. The theoretically calculated cross section data for the reaction were as displayed in Table 4.3 together with experimentally given data from EXFOR for each energy

4.3.3 Comparison between experimental data and obtained data in this research

Table 4.3: Excitation function for the reaction $^{134}Ba(n,p)^{134}Cs$

$E_n(MeV)$	$\sigma - Experimental(mb)$	$\sigma - Theoretical(mb)$
1.28552	0	0
2.04011	0	0
3.04757	0	0
4.05504	0.0003242	0.01863
5.0625	0.006355	0.1362
6.06996	0.02641	0.4314
7.07743	0.07051	0.05452
8.084889	0.1736	0.1714
9.09235	0.8854	0.3276
10.0998	0.8854	0.885
11.1073	1.694	1.7512
12.1147	2.869	2.975
13.1222	4.402	5
14.1297	6.215	7.56
15.1371	8.177	9.8
16.1446	10.07	12.3
17.1521	11.63	14
18.1595	12.65	15.4
19.167	13.02	16
20.1744	12.8	15

Table 4.3 shows for the first three given neutron energies the experimental and theoretical values of the cross section values are zero. For the higher values of the given neutron energies calculated values of cross section slowly deviate from experimental values. For the neutron energies of 7.07743MeV and 8.084889MeV calculated values of cross section are less than experimental values. There is about 2.98 deviation of values between the theoretical and experimental values at the 19.167MeV to the maximum. From this result one can conclude that COMPLET code calculation data approaches the experimental value for the reaction on energy range 1 to 20MeV.

Figure 4.3: Excitation function for the reaction $^{134}Ba(n,p)^{134}Cs$

4.4 Excitation function of the reaction $^{135}Ba(n,p)^{135}Cs$

4.4.1 Experimental Excitation Function

Neutron activation cross sections have been measured systematically at energy range from 13.3 to 15.0 MeV utilizing the fusion neutronics source (FNS) facility in order to provide substantial nuclear data required in the fusion reactor nuclear design. Up to now,110 cross section data for reactions of $(n,p), (n,n'p), (n,\alpha)$ and $(n,2n)$ in 26 elements including major structural materials of iron, nickel, chromium, titanium,

molybdenum,etc. were measured in a unified experimental condition [13].

4.4.2   Theoretical Excitation Function

Theoretically, cross section values were calculated using COMPLET code with neutron energies. The theoretically calculated cross section data for the reaction were as displayed in Table 4.4 together with experimentally given data in EXFOR for each energy.

4.4.3   Comparison between experimental data and obtained data in this research

Table 4.4: Excitation function for the reaction $^{135}Ba(n,p)^{135}Cs$

$E_n(MeV)$	$\sigma - Experimental(mb)$	$\sigma - Theoretical(mb)$
13.34	0.24	0.231
13.57	0.216	0.212
13.76	0.53	0.24
13.99	0.297	0.27
14.23	0.262	0.244
14.44	0.293	0.28
14.68	0.307	0.266
14.95	0.36	0.305

As it is possible to understand from both the given Table 4.4 and Figure 4.4, as neutron entered to ^{135}Ba radio active cesium ^{135}Cs was obtained. The theoretical reaction cross section value is best nearest to experimental value at 13.57MeV neutron energy. However, theoretical cross section value is some what far from experimental value at 13.76MeV neutron energy. All calculated values of the cross section values are less than experimental values of cross section for the neutron energies 13.34 to

14.95MeV. From the given Table and Figure one conclude that a presence of a good agreement between the two values i.e., theoretical values and experimental values as compared to other values calculated for the reactions in this research.
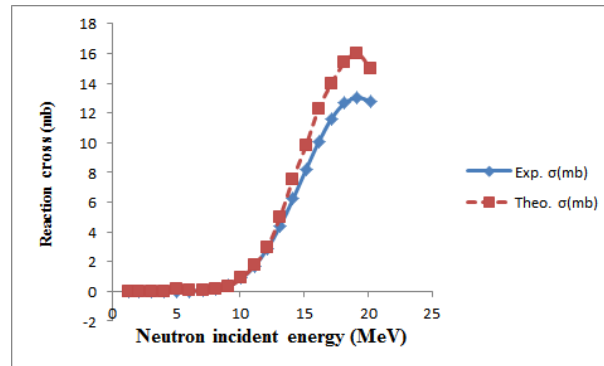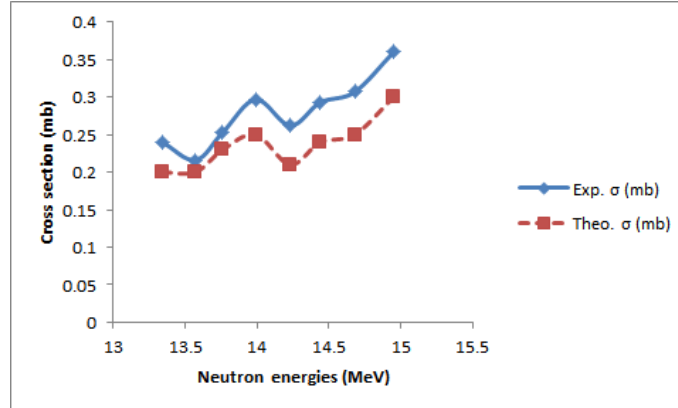

Figure 4.4: Excitation function for the reaction $^{135}Ba(n,p)^{135}Cs$

4.5 Excitation function of the reaction $^{136}Ba(n,p)^{136}Cs$

4.5.1 Experimental Excitation Function

Y.Ikeda, C.Konno, K.Oishi, T.Nakamura, H.Miyade, K.Kawade, H.Yamamoto, T.Katoh in their work which was entitled as Activation cross section measurements for fusion reactor structural materials at neutron energy from 13.3 to 15.0MeV using (FNS) facility experimentally they calculated the cross section values from 13.33MeV to 14.94MeV for the reaction [13].

4.5.2 Theoretical Excitation function

Using Fortran-77 based nuclear code which is called COMPLET the calculation of cross section values were made for the given neutron energies.

4.5.3 Comparison between experimental data and obtained data in this research

Table 4.5: Excitation function for the reaction $^{136}Ba(n,p)^{136}Cs$

$E_n(MeV)$	$\sigma - Experimental(mb)$	$\sigma - Theoretical(mb)$
13.33	2.9	3.873
13.57	2.96	4
13.99	5.94	5.492
14.44	5.81	5.731
14.68	8	6.89
14.94	6.93	7

As it is possible to understand from both the given Table 4.5 and Figure 4.5 the theoretical cross section values are very close to experimental value at 14.94MeV and 14.44MeV neutron incident energies. The graph of the excitation function plotted also shows that to some extent the theoretical and experimental values cross section are close to each other. At two values of neutron energies i.e., 13.57MeV and 14.68MeV the theoretically obtained reaction cross section value are some what far from experimental values of reaction cross sections. The calculated values of the reaction cross section are less than experimental values for the neutron energies of 13.99MeV, 14.44MeV and 14.68MeV. However, experimental values are less than calculated values for the 13.33MeV and 14.93MeV of neutron energies. From both Table 4.5 and Figure 4.5 one can conclude that COMPLET code calculation data approaches the experimental value for the reaction on energies 13.33MeV, 13.57MeV, 13.99MeV, 14.44MeV, 14.68MeV and 14.94MeV.
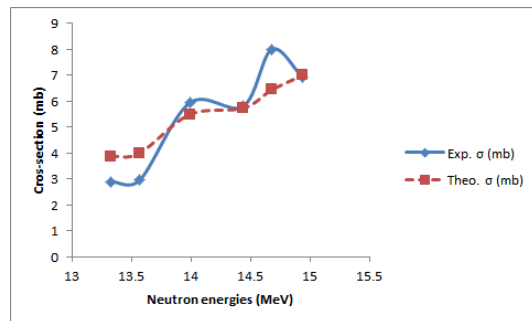
Figure 4.5: Excitation function for the reaction $^{136}Ba(n,p)^{136}Cs$

Chapter 5

Conclusion

In this work, the reaction cross section of five nuclear reactions : $^{134}Ba(n, 2n)^{133}Ba$, $^{136}Ba(n, 2n)^{135}Ba$, $^{134}Ba(n, p)^{134}Cs$, $^{135}Ba(n, p)^{135}Cs$ and $^{136}Ba(n, p)^{136}Cs$ were studied. The theoretical data obtained in this work were based on calculations using a nuclear reaction computer program, COMPLET. From the result of the output of the code compared with the available experimental data, the following conclusions have been drawn.

- COMPLET code calculation data approaches the experimental value for the reaction $^{134}_{56}Ba(n, 2n)^{133}_{56}Ba$ on energy range 13 to 15MeV.

- Theoretically calculated values of cross section with COMPLET code and experimental values are in a good agreement for the reaction $^{136}_{56}Ba(n, 2n)^{135}_{56}Ba$ on energy range 13 to 15MeV.

- Calculated values of cross section using COMPLET code related to the experimental values for the reaction $^{134}_{56}Ba(n, p)^{134}_{55}Cs$ on energy range 1 to 20MeV.

- COMPLET code based calculated data agrees with the experimental data for the reaction $^{135}_{56}Ba(n, p)^{135}_{55}Cs$ on energy range 1 to 20MeV.

- Theoretically calculated cross section data using COMPLET code meets the experimental data for the reaction $^{136}_{56}Ba(n,p)^{136}_{55}Cs$ for energy range 1 to 20MeV.

Bibliography

[1] M.E Korkmaz, M. M. Yigit, and O. Agar. Excitation functions of neutron induced nuclear reactions for ^{59}co nucleus using different level density models. *Acta Physica polonica*, 132(3), 2017.

[2] Robert E. Krebs. *The History and Use of Our Earth's Chemical Elements.* Greenwood Press, 2 edition, 2006.

[3] M. Blatt John and F. Weisskopf Victor. *Theoretical Nuclear Physics.* Springer, 1979.

[4] C.A. Bertulani. Nuclear reaction. *Wiley Encyclopedia of Physics*, 2009.

[5] A. M. Lane and R. G. Thomas. R-matrix theory of nuclear reactions. *Reviews of modern Physics.*

[6] Peter Reimer. *Neutron induced reactions leading to activation products: selected cases relevant to development of low activation materials, transmutation and hazard assessment of nuclear wastes.* PhD thesis, zu Koln, February 2002.

[7] Fatima Salman Koki Idris Ahmad, Yahya Ibrahim Yola. Evaluation of excitation functions of reactions used in production of some medical radioisotopes. *International Journal of Medical Physics, Clinical Engineering and Radiation Oncology*, 6:290–303, August 2017.

[8] Kenneth S.Krane. *Introductory Nuclear Physics*. Kim Hup Lee, 1987.

[9] Irving Kaplan. *Nuclear Physics*. Addison-Wesley, 1977.

[10] Riccardo Bevilacqua. *Neutron induced light-ion production from iron and bismuth at 175 MeV*. PhD thesis, Uppsala University, January 2010.

[11] Anthony J.Baratta John R.Lamarsh. *Introduction to Nuclear Engineering*. Addison- Wesley, 3 edition, 1983.

[12] A. J Koning and M.C. .Duijvestijn. A global pre-equilibrium analysis from 7 to 200 mev based on the optical model potential. *ELSEVIER*, 744, September 2004.

[13] KojiO Ishi Tomoo Nakamura Hiro kimiyade Kiyoshi Kawade Hiroshi Yamamoto Yujiro Ikeda, Chikara Konno and Toshio Katoh. Activation cross section measurements for fusion reactor structural materials at neutron energy from 13.3 to 15.0mev using fns facility. *Japan Atomic Energy Research Institute*, 1988.

[14] Eyyup Tel Halide Sahan, Muhittin Sahan. Calculations of (n,2n) reaction cross sections for barium isotopes from 5 to 20 mev. volume 154, Turkey, 2017. TES-NAT.

[15] B. Strohmaier, M. Uhl, and W.K. Matthes. Application of nuclear reaction models for neutron nuclear data evaluation: Statistical and optical model calculations for $134138ba$. *Nuclear Science and Engineering*, 65.

Annex

CODE COMPLET

The Code COMPLET is a FORTRAN 77 based computer code and is a nuclear reaction code used to simulate virtual beam by generating energy from a few MeV to a number of MeV. The computational code was commanded in the following manner in the For tran Compiler.

CARD 1 General Input Data

AP   Projectile Mass Number

AT   Target Mass Number

ZP   Projectile Charge

ZT   Target Charge

QVAL Reaction Q Value = AP+AT-ACN.   =0: Calc. From M and S Mass Formula.

=1: Calculated from mass excesses of 1990 nuclear wallet cards

PLD   Level density parameter 'a', a=ACN/PLD. =0: a=ACN/8.

CLD   ratio of single particle level densities $\frac{af}{an} = 0$: $\frac{af}{an}$=1.0

BARFAC multiplies the rotating drop fission barrier by this value.

=0: BARFAC = 1.

ROTFAC   multiplies the rotational energy by this value.

=0: ROTFAC=1.

RO   critical temperature above onset of retarded fission

GI   nuclear friction parameter from EQ. deformation to saddle

G0   nuclear friction parameter from saddle to scission point

NA   number of nuclides of each Z to be included in calculation. Up to 21 neutrons

may be emitted (maximum NA=22)

NZ   number of Z to be calculated in the emission process. Up to 8 protons may be emitted (maximum NZ=9) for correct PE calculations binding energies are calculated for all nuclei with IZ, IA $<= 5$ (17.7.91)

MC   shell correction option for masses subroutine.

MC=0,shell corr.

MC=1, no shell corr.

MC=2, BE values will be supplied as input.

MC > 2, BE-values are calculated from 1990 nuclear wallet cards

MP   pairing correction to masses. =0:no correction;

=1:pairing term

=2: masses are from nuclear wallet cards;

=3: pairing correction in masses,

NOTE: changes are not corrections in only level densities.

IPA   pairing corrections in level densities;IP=-1,no corrections,

IP $= 0$ standard correction i.e. multiplier $= 12$

If IPA >0 multiplier is IPA

M3   number and type of particles to be emitted from each nuclide.

If =1: n only; =2: n and p; =3 or =0: n,p and alpha; =4: n,p,alpha and deuteron, =5: n, p, alpha, deuteron and triton; =6: n, p, alpha, deuteron, triton and helion (3He); =7: as before incl. Gammas. calculations until gamma emission is finished, important for isomeric ratio calculations.

INVER inverse cross section param.

=0: user will supply;

=1: results by O.M. subroutines as in ALICE/85/300, + PEREY'S t,3He O.M., d,t,3He O.M.,

=2: O.M. for n,p as in old ALICE, a as in PRC49,2136 + PEREY'S d,t,3He O.M.,

=3: sharp cut off values for inverse cross-sections.

IKE   If =1: no particle spectra will be printed;

If =2: equilibrium spectra for each nuclide will be printed !!!;

If =3: only PE- spectra will be printed;

If = 5: PE plus summed equilibrium spectra will be (separately) printed; if = 4: as 2+3 !!!

If IKE = -2 to -5: reduced output with spectra as IKE = ABS(IKE) (yields are printed after negative energy input)

If IKE <= 0 or IKE >= 6 most reduced output

IPCH   =1: inverse cross sections will be readout for possible future use in separate output file. =0: or NE from 1, no printout.

KPLT   number of decades to be plotted as excitation function on line printer. If KPLT=0: no plotting

CARD 2 Title Card - 80 Columns

If MC = 2 on card1, read user supplied n, p, alpha, deuteron triton and helion binding energies here, format(4F10.5) for IA=1 to NA, IZ=1 to NZ if INVER = 0 on card1, read n, p, alpha, deuteron, triton, helion and gamma inverse cross sections here. format is (7E10.5) in ascending channel energy, first value = 0.1 MeV, incremented by 1 MeV, 48 values per particle type in sequence n, p, a, d, t, ^3He and gamma depending on value of M3.

CARD 3 Energy and CN and PE Options

EKIN   projectile kinetic energy in the laboratory system.

if =0.: a new problem will begin at CARD1.

if <0.: previously calculated excitation functions will be printed (if not KPLT=0, EKIN values were run in ascending order they are plotted). If ekin=0. On two successive cards, a normal exit will occur for negative target mass on CARD1.

RCSS =0: reaction cross section is calculated from subroutine (for pi-induced reactions: if RCSS(input)=0., RCSS = 100 mb) > 0: number of T(l) values to be read from the next card if < 0: calculated rcss is multiplied by this value times -0.01

JCAL   type of calculation option. =1: Weisskopf,

=2: s-wave with liquid drop moment of inertia,

=3: s-wave with rigid body,

=0: calc for all partial wave including fission and full angular momentum coupling up to delta l=12 (for gammas delta l=0,1). (previous option JCAL = -1 is no more existing).

JFRAC   direct-semidirect capture gamma ray estimate: < 0 no emission, > 0 approach of KALKA, = 0 simple approach with initial exciton-number =1 for p,n.

JUPPER   JUPPER LT 0, Blann-Reffo type PE-gamma-emission using s.p. state densities instead of 1P1H two-partcile densities.

Normalization factor = 1/GIANT with GIANT=ABS(JUPPER)/100.

For JUPPER GE 0 photo absorption yield normalized to 1P1H state normalization factor = GIANT with GIANT=ABS(JUPPER)/100.

JANG   JANG+1 = maximum number of contributing incoming partial waves.

Usually use the maximum: JANG = 99. Otherwise, JANG can be used for cutoff on l-values provided by subroutines over1 and 2.

All additional parameters on this card are for pre-compound options. Put TD-value to zero if no PE calculation is wanted

IJ   if = 1 (or 3): GP=GN=3/4*A/POT

if = 0 (or 2): GP=3/2*Z/POT,GN=3/2*(A-Z)/POT

TD   initial exciton number=P+H.

EX1   initial excited neutron number.

EX2   initial excited proton number.

EX3   initial alpha particle exciton number

POT   fermi energy in MeV

If = 0.: POT is calculated from nucl. Matter value = 37.8 MeV

AV   if = 0.:optical model mean free paths are used in routine MFP. Not to be used above 55 MeV. If AV = 1: nucleon-nucleon mean free paths are used in NUCMFP.

ALF   probability that newly created exciton particle from 1st stage exciton gets an alpha particle in the second stage. (1-ALF): complementary probability if ALF > 1 calculation for two initial exciton numbers

a) ATD=TD-3 (min. 1.5) AEX1=AEX2=0, AEX3=2.;ATD=TD-6 for TD¿9 with weight ULF=INT(ALF)/100

b) weight=(1-ULF), with initial EXC. Numbers.

CMFP   mean free paths are multiplied by CMFP. If CMFP=0.: multiplier is 1.0

GDO   critical angular momentum. GDO > 0: partial waves with $l >$ GDO are not taken into account in the line of isotone cross-sections while cross-sections for partial waves with $l >$ GDO are accounted for in the line below.

N.B. for GDO <= +0.5 no cut-off.

JIMMA UNIVERSITY
COLLEGE OF NATURAL SCIENCES
PERFORMANCE CERTIFICATE FOR MASTER'S DEGREE

Name of Student: **Kebede Shogile**   ID No. **RM1196/09**

Graduate Program: **Regular, MSc.**

1. Course Work Performance

Course Code	Course Title	Cr. hr	Score (%)	Rank **	Remark
Phys 799	**MSc. Thesis**	**6**	88.5	**	

** Excellent, Very Good, Good, Satisfactory, Fail.

Thesis Title

Excitation Function of Neutron Induced Reaction on Barium Isotopes for Neutron Energies Below 20MeV

2. Board of Examiners decision Mark $\times$ in one of the boxes. Promoted $\boxed{\times}$ Failed $\square$

   If failed, give reasons and indicate plans for re-examination.

   _____

   _____

3. Approved by: Name and Signature of members of the examining Board, and Deans, SGS

Committee member	Name	Signature	Date
Chairman	_____	_____	_____
External Examiner	_____	_____	_____
Internal Examiner	_____	_____	_____
Major Advisor	_____	_____	_____

_____   _____   _____
Department Head   Signature   Date

School of Graduate Studies
Jimma University
College of Natural Sciences
MSc. Thesis Approval Sheet

We the undersigned, number of the Board of Examiners of the final open defense by **Kebede Shogile**, have read and evaluated his thesis entitled "**Excitation Function of Neutron Induced Reaction on Barium Isotopes for Neutron Energies Below 20MeV**" and examined the candidate. This is therefore to certify that the thesis has been accepted in partial fulfilment of the requirements for the degree of Master of Science in **Physics (Nuclear Physics)**.

Name of the Chairperson	Signature	Date

Name of Major Advisor	Signature	Date

Name of Internal Examiner	Signature	Date

Name of External Examiner	Signature	Date

SCHOOL OF GRADUATE STUDIES

DECLARATION

I hereby declare that this MSc thesis is my original work and has not been presented for a degree in any other University and that all source of materials used for the thesis have been duly acknowledged.

Name: Kebede Shogile

Signature: _____
email: kebedeshogile98@gmail.com

This Msc thesis has been submitted for examination with my approval as University advisor.

Name: Dr.Teklemariam Tessema

Signature: _____

Place and date of submission:

Department of Physics

Jimma University

June, 2018